

Research Article

QSPR Study and Distance-Based New Topological Descriptors of Some Drugs Used in the COVID-19 Treatment

Vignesh Ravi ¹, Natarajan Chidambaram,² Özge Çolakoglu ³, Hanan Ahmed ⁴,
Subhasri Jaganathan,² and Jayasri Jaganathan²

¹Division of Mathematics, School of Advanced Sciences, Vellore Institute of Technology, Chennai, India

²Department of Mathematics, Srinivasa Ramanujan Centre, SASTRA Deemed to be University, Kumbakonam, India

³Mathematics Department, Science and Art Faculty, Mersin University, Mersin 33343, Turkey

⁴Department of Mathematics, Ibb University, Ibb, Yemen

Correspondence should be addressed to Hanan Ahmed; hananahmed1a@gmail.com

Received 18 November 2022; Revised 28 February 2023; Accepted 15 March 2023; Published 25 April 2023

Academic Editor: G. Muhiuddin

Copyright © 2023 Vignesh Ravi et al. This is an open access article distributed under the Creative Commons Attribution License, which permits unrestricted use, distribution, and reproduction in any medium, provided the original work is properly cited.

In chemistry and medical sciences, it is essential to study the chemical, biological, clinical, and therapeutic aspects of pharmaceuticals. To save time and money, mathematical chemistry focuses on topological indices used in quantitative structure-property relationship (QSPR) models to predict the properties of chemical structures. The COVID-19 pandemic is widely recognized as the greatest life-threatening crisis facing modern medicine. Scientists have tested various antiviral drugs available to treat COVID-19 disease, and some have found that they help get rid of this viral infection. Antiviral drugs such as Arbidol, chloroquine, hydroxychloroquine, lopinavir, remdesivir, ritonavir, thalidomide, and theaflavin are used to treat COVID-19. In this paper, reformulated leap Zagreb indices are introduced. Then, the reformulated leap Zagreb indices, leap eccentric connectivity indices, and reformulated Zagreb connectivity indices of these antiviral drugs are calculated. Curvilinear and multilinear regression models predicting the physicochemical properties of these antiviral drugs in terms of proposed indices are obtained and analyzed. The findings and models of this study will shed light on new drug discoveries for the treatment of COVID-19.

1. Introduction

Chemical graph theory is the mathematical modeling of molecules. It is a branch of graph theory that studies all of the effects of connection in a chemical network. It focuses on the topological indices. A topological index (molecular descriptor) is a mathematical measure of chemical compounds represented as molecular graphs. It is used in quantitative structure-activity relationship (QSAR) and quantitative structure-property relationship (QSPR) studies to model the physicochemical, pharmacological, toxicological, biological, and other aspects of chemical compounds in theoretical chemistry. A molecular graph is the skeleton of a chemical structure that does not contain hydrocarbons. The vertices of the molecular graph represent the atoms of the chemical structure, and the edges represent the bonds of the chemical structure [1].

In the development of pharmaceutical drugs, a compound's physicochemical characteristics and biological activities are critical. Without the use of laboratories, the topological index, a traditional aid of chemical graph theory, can be used to predict these features. Many researchers are working on quantitative structure-property relationship (QSPR) analysis of various chemical substances ([2, 3]) since it is a more cost-effective method of testing than testing in a wet lab.

The COVID-19 global epidemic is widely regarded as the greatest life-threatening crisis that modern medicine has ever faced, especially in comparison to earlier infectious diseases. Medical researchers [4–8] have been working around the clock to find drugs that can save lives and even prevent them from being ill. It is necessary to produce drugs in the shortest time and at the least cost. Therefore, equations that will help the production of new drugs have been

obtained by using topological indices with existing drugs. Researchers have recently been working on topological indices and COVID-19 medicines [2, 9–12]. Also, the following articles are noteworthy in the research of drugs repurposed against SARS-CoV-2. Nandi et al. [13] studied various US-FDA-approved chemotherapeutics repositioned to combat COVID-19 spread. Nandi et al. [14] performed a docking analysis of 34 drugs which include antivirals and antimalarials and discussed extensively the mode of interactions of these ligands towards the COVID-19 protease target. Also, Nandi et al. [15] extended the study of their previous regression model that correlates the dock scores of six drugs to a regression model that explores the potential mechanism of action of antiviral and antimalarial drugs in combating COVID-19. Some of drugs used in COVID-19 treatment are Arbidol, chloroquine, hydroxychloroquine, lopinavir, remdesivir, ritonavir, thalidomide, and theaflavin. The chemical structure (molecular graphs) of these drugs is given in Figures 1 and 2.

Recently, the molecular graph-based topological indices have been taken into the quantitative structure-property activity relationship modeling of many anti-COVID-19 compounds. There are about 1000 topological descriptors available in the literature. Among those indices, distance-based indices attract many researchers, and most of these indices behave nicely when studying the QSPR/QSAR analysis of various drugs. Nagarajan et al. [16] have done QSPR modeling of status-based indices with COVID-19 drugs and obtained noteworthy results. Çolakoğlu [17] analyzed QSPR modeling with topological indices of some potential drugs against COVID-19. Nandi et al. [18] performed QSAR of SARS-CoV-2 main protease inhibitors by applying theoretical descriptors. In 2017, Naji et al. [19] introduced and studied a new set of distance-based topological descriptors called “leap Zagreb indices.” Since their introduction, these indices attract several researchers, and as a result, the research articles pertaining to these indices are growing exponentially. Shao et al. [20] found some interesting bounds on leap Zagreb indices of trees and unicyclic graphs. Most recently, Alsinai et al. [21] introduced the fourth leap Zagreb index of graphs and obtained a set of significant results. Zhu et al. [22] investigated the third leap Zagreb index for trees. In [23], Raza studied the leap Zagreb connection index of some network models. Raza [24] computed leap Zagreb connection indices for benzenoid systems.

The first, second, and third leap Zagreb indices are defined, respectively, as follows:

$$LM_1(G) = \sum_{v \in V(G)} d_2(v)^2, \quad (1)$$

$$LM_2(G) = \sum_{uv \in E(G)} d_2(u)d_2(v), \quad (2)$$

$$LM_3(G) = \sum_{v \in V(G)} d(v)d_2(v), \quad (3)$$

where $d(v)$ and $d_2(v)$ represent, respectively, the degree and 2-degree of a vertex v in G . The 2-degree of a vertex v is the number of vertices that are of distance two from v in G .

Sharma et al. [25] introduced leap eccentric connectivity index of G which is defined as

$$LEC(G) = \sum_{v \in V(G)} d_2(v)e(v). \quad (4)$$

Let $\tau(v)$ denote the connection number of a vertex v in graph G , that is, the 2-degree of the vertex v in G (the number of vertices which are distance two apart from the vertex v).

We introduce reformulated leap Zagreb indices which are a new set of topological indices:

$$RZC_1(G) = \sum_{e \in E(G)} \tau(e)^2, \quad (5)$$

where $e = uv$ and $\tau(e) = \tau(u) + \tau(v) - 2$.

$$RZC_2(G) = \sum_{e\tilde{f}} \tau(e)\tau(f), \quad (6)$$

where $e\tilde{f}$ represents the adjacent edges e and f in G .

$$RZC_3(G) = \sum_{e \in E(G)} \deg(e)\tau(e), \quad (7)$$

where $e = uv$ and $\deg(e) = \deg(u) + \deg(v) - 2$.

For further results about these descriptors, one may refer to [20, 26–33].

In this paper, reformulated leap Zagreb indices are introduced. The reformulated leap Zagreb indices and leap topological indices of some drugs used in COVID-19 treatment are computed for use in QSPR models. Curvilinear and multilinear regression models are obtained for some physicochemical properties of these drugs. Finally, these models are compared and the best estimator index and models are obtained.

2. Methodology and Analysis

To compute our results, we use the method of edge partitions with the help of graph-theoretical tools and a method of computing the 2-degree (or connection number) and leap eccentricity of a vertex.

2.1. Vertex Partitions to Compute Leap Zagreb Indices for COVID-19 Drugs. The 2-distance degrees and eccentricities for every $u \in V$ in molecular graphs of some drugs used in the treatment of COVID-19 disease are given in the tables below. Table 1 shows the 2-distance degree and eccentricity-based vertex partition of the drugs considered.

2.2. Edge Partitions to Compute Leap Zagreb Indices. Tables 2 and 3 show the 2-distance degree partition of drugs considered.

2.3. (Degree, 2-Degree) Vertex Partition to Compute Leap Zagreb Indices. Table 4 shows the degree and 2-degree vertex partition of the considered drugs.

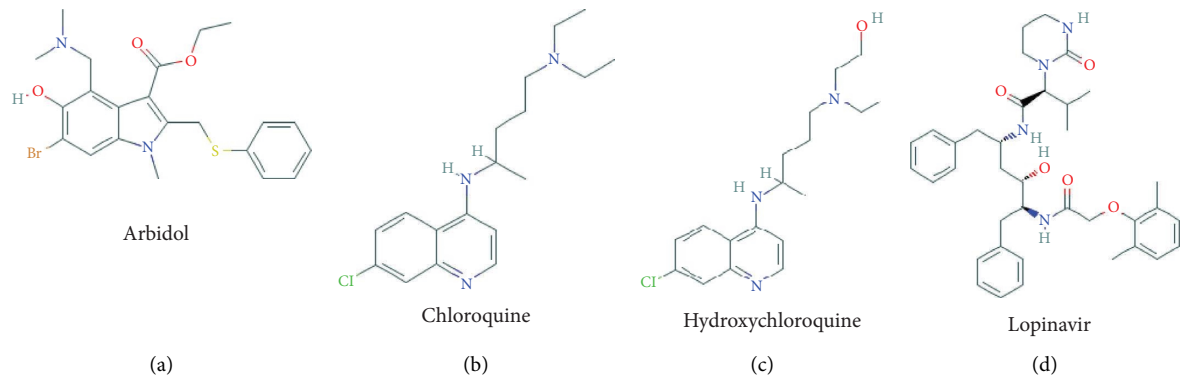


FIGURE 1: The molecular structure of (a) Arbidol, (b) chloroquine, (c) hydroxychloroquine, and (d) lopinavir [10].

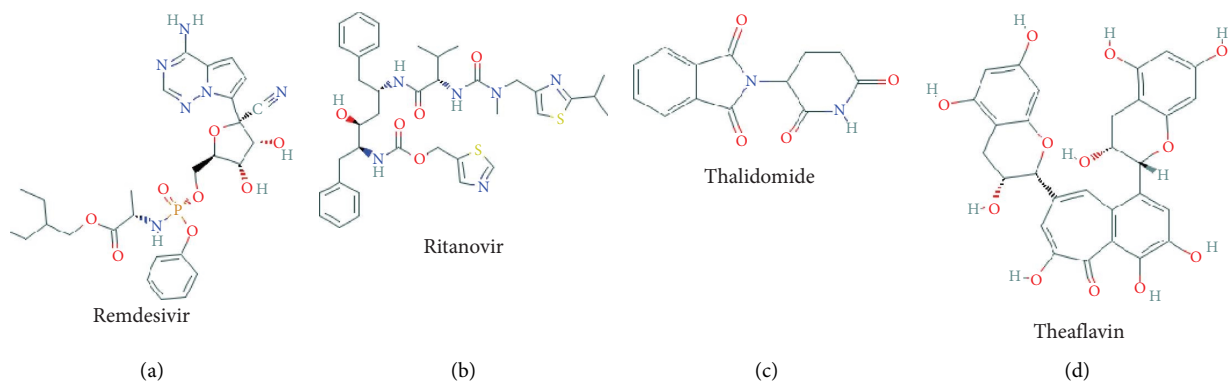


FIGURE 2: The molecular structure of (a) remdesivir, (b) ritonavir, (c) thalidomide, and (d) theaflavin [10].

TABLE 1: The 2-distance degree and eccentricity-based vertex partition.

| Drugs | 1 | 2 | 3 | 4 | 5 | 6 |
|-----------------------|---|----|----|----|---|---|
| Arbidol A | 3 | 9 | 8 | 4 | 3 | 2 |
| Chloroquine C | 2 | 8 | 7 | 4 | 1 | — |
| Hydroxychloroquine HC | 3 | 7 | 8 | 4 | 1 | — |
| Lopinavir L | — | 19 | 18 | 6 | 2 | 1 |
| Remdesivir Re | 2 | 11 | 17 | 3 | 7 | 1 |
| Ritonavir Ri | — | 20 | 19 | 10 | 1 | — |
| Thalidomide T | — | 7 | 6 | 2 | 3 | 1 |
| Theaflavin Th | — | 12 | 6 | 16 | 6 | 1 |

TABLE 2: 2-degree edge partition.

| Drugs | (1, 1) | (1, 2) | (1, 3) | (1, 4) | (2, 2) | (2, 3) | (2, 4) | (2, 5) | (2, 6) |
|-------|--------|--------|--------|--------|--------|--------|--------|--------|--------|
| A | 1 | 2 | 1 | 1 | 2 | 4 | 2 | — | — |
| C | — | 2 | — | — | 2 | 8 | 2 | — | — |
| HC | 1 | 1 | 1 | — | 2 | 7 | 2 | — | — |
| L | — | — | — | — | 8 | 14 | 1 | — | 1 |
| Re | — | 2 | — | — | 2 | 9 | 1 | 1 | — |
| Ri | — | — | — | — | 10 | 11 | 2 | 1 | — |
| T | — | — | — | — | 2 | 5 | 2 | — | — |
| Th | — | — | — | — | 2 | 6 | 6 | — | — |

2.4. Vertex Partitions to Compute Leap Eccentric Connectivity Index for COVID-19 Drugs. Tables 5–9 show the 2-degree and eccentricity-based vertex partition of the considered drugs.

2.5. Edge Partitions to Compute the Reformulated Leap Zagreb Index RZC_1 for COVID-19 Drugs. Table 10 shows the edge partition of the considered drugs with respect to RZC_1 index.

TABLE 3: 2-degree edge partition (continued).

| Drugs | (3, 3) | (3, 4) | (3, 5) | (3, 6) | (4, 4) | (4, 5) | (4, 6) | (5, 5) | (5, 6) | (6, 6) |
|-------|--------|--------|--------|--------|--------|--------|--------|--------|--------|--------|
| A | 5 | 2 | 1 | 1 | — | 5 | — | — | 3 | 1 |
| C | 2 | 2 | 1 | — | 2 | 2 | — | — | — | — |
| HC | 3 | 2 | 1 | — | 2 | 2 | — | — | — | — |
| L | 8 | 8 | 5 | 1 | 2 | — | — | — | 1 | — |
| Re | 9 | 3 | 8 | 1 | 1 | 2 | — | 3 | 2 | — |
| Ri | 11 | 13 | 1 | — | 3 | 1 | — | — | — | — |
| T | 2 | — | 4 | — | — | 2 | 2 | 1 | 1 | — |
| Th | — | 8 | 4 | — | 6 | 9 | 2 | 2 | 1 | — |

TABLE 4: (Deg, 2-deg)-partition.

| Drugs | (1, 1) | (1, 2) | (1, 3) | (2, 1) | (2, 2) | (2, 3) | (2, 4) | (2, 5) | (3, 1) | (3, 2) | (3, 3) | (3, 4) | (3, 5) | (3, 6) | (4, 5) |
|-------|--------|--------|--------|--------|--------|--------|--------|--------|--------|--------|--------|--------|--------|--------|--------|
| A | 1 | 6 | — | 1 | 3 | 5 | 2 | — | 1 | — | 3 | 2 | 3 | 2 | — |
| C | 2 | 2 | — | — | 4 | — | 2 | — | — | 2 | 1 | 2 | 1 | — | — |
| HC | 2 | 2 | — | 1 | 3 | 7 | 2 | — | — | 2 | 1 | 2 | 1 | — | — |
| L | — | 8 | — | — | 9 | 10 | 5 | — | — | 2 | 8 | 1 | 2 | 1 | — |
| Re | 2 | 5 | 2 | — | 6 | 9 | 1 | 3 | — | — | 5 | 3 | 3 | 1 | 1 |
| Ri | — | 9 | — | — | 8 | 11 | 8 | — | — | 3 | 8 | 2 | 1 | — | — |
| T | — | 4 | — | — | 2 | 5 | — | — | — | 1 | 1 | — | 3 | 1 | — |
| Th | — | 10 | — | — | — | — | 11 | — | — | 2 | 6 | 5 | 6 | 1 | — |

TABLE 5: 2-degree and eccentricity-based vertex partition.

| Drugs | (1, 10) | (1, 11) | (1, 13) | (1, 14) | (1, 18) |
|-------|---------|---------|---------|---------|---------|
| A | 1 | 2 | — | — | — |
| C | — | — | 2 | — | — |
| HC | — | — | 2 | — | — |
| L | — | — | — | — | — |
| Re | — | — | — | — | 2 |
| Ri | — | — | — | — | — |
| T | — | — | — | — | — |
| Th | — | — | — | — | — |

TABLE 6: 2-degree and eccentricity-based vertex partition (continued).

| Drugs | (2, 7) | (2, 8) | (2, 9) | (2, 10) | (2, 11) | (2, 12) | (2, 13) | (2, 14) | (2, 15) | (2, 16) | (2, 17) | (2, 18) | (2, 19) | (2, 20) | (2, 21) | (2, 22) |
|-------|--------|--------|--------|---------|---------|---------|---------|---------|---------|---------|---------|---------|---------|---------|---------|---------|
| A | — | 1 | 1 | — | 4 | 3 | — | — | — | — | — | — | — | — | — | — |
| C | 1 | 1 | 1 | 1 | — | 3 | 1 | — | — | — | — | — | — | — | — | — |
| HC | 1 | 1 | 1 | — | 1 | 1 | 1 | 1 | — | — | — | — | — | — | — | — |
| L | — | — | — | 1 | — | 1 | 1 | 3 | 4 | 3 | 4 | 2 | — | — | — | — |
| Re | — | — | — | — | — | — | 2 | 4 | 1 | — | 3 | 1 | — | — | — | — |
| Ri | — | — | — | — | — | — | 1 | 1 | 3 | 3 | 3 | 1 | 2 | 1 | 1 | 4 |
| T | 3 | 1 | 3 | — | — | — | — | — | — | — | — | — | — | — | — | — |
| Th | — | — | — | 1 | 2 | 3 | — | 2 | 4 | — | — | — | — | — | — | — |

TABLE 7: 2-degree and eccentricity-based vertex partition (continued).

| Drugs | (3, 6) | (3, 7) | (3, 8) | (3, 9) | (3, 10) | (3, 11) | (3, 12) | (3, 13) | (3, 14) | (3, 15) | (3, 16) | (3, 17) | (3, 18) | (3, 19) | (3, 20) | (3, 21) |
|-------|--------|--------|--------|--------|---------|---------|---------|---------|---------|---------|---------|---------|---------|---------|---------|---------|
| A | 1 | 2 | 2 | 3 | — | — | — | — | — | — | — | — | — | — | — | — |
| C | — | — | 1 | 1 | 2 | 3 | — | — | — | — | — | — | — | — | — | — |
| HC | — | — | 1 | — | 2 | 2 | 3 | — | — | — | — | — | — | — | — | — |
| L | — | — | — | 1 | — | 1 | 1 | — | 5 | 3 | — | 4 | 3 | — | — | — |
| Re | — | — | — | — | 2 | 1 | 2 | 3 | 2 | 2 | 3 | 1 | 1 | — | — | — |
| Ri | — | — | — | — | — | — | 2 | — | 2 | 4 | 1 | 1 | 4 | 2 | 2 | 2 |
| T | 2 | 2 | 2 | — | — | — | — | — | — | — | — | — | — | — | — | — |
| Th | — | — | — | — | 1 | 3 | — | — | 2 | — | — | — | — | — | — | — |

TABLE 8: 2-degree and eccentricity-based vertex partition (continued).

| Drugs | (4, 6) | (4, 7) | (4, 8) | (4, 9) | (4, 10) | (4, 11) | (4, 12) | (4, 13) | (4, 14) | (4, 15) | (4, 16) | (4, 17) | (4, 18) | (4, 19) | (4, 20) |
|-------|--------|--------|--------|--------|---------|---------|---------|---------|---------|---------|---------|---------|---------|---------|---------|
| A | — | 1 | — | 1 | 2 | — | — | — | — | — | — | — | — | — | — |
| C | — | 1 | 1 | — | 1 | 1 | — | — | — | — | — | — | — | — | — |
| HC | — | — | 1 | 1 | — | 1 | 1 | — | — | — | — | — | — | — | — |
| L | — | — | — | — | 2 | 2 | 2 | — | — | — | — | — | — | — | — |
| Re | — | — | — | 1 | — | 1 | 1 | — | — | — | — | — | — | — | — |
| Ri | — | — | — | — | — | 1 | — | 2 | 1 | — | 2 | 1 | — | 1 | 1 |
| T | 2 | — | — | — | — | — | — | — | — | — | — | — | — | — | — |
| Th | — | — | 1 | 2 | 3 | 2 | 4 | 2 | — | 2 | — | — | — | — | — |

TABLE 9: 2-degree and eccentricity-based vertex partition (continued).

| Drugs | (5, 5) | (5, 6) | (5, 7) | (5, 8) | (5, 9) | (5, 10) | (5, 11) | (5, 12) | (5, 13) | (5, 15) | (5, 16) | (6, 5) | (6, 7) | (6, 8) | (6, 9) | (6, 14) |
|-------|--------|--------|--------|--------|--------|---------|---------|---------|---------|---------|---------|--------|--------|--------|--------|---------|
| A | — | 1 | — | 1 | 1 | — | — | — | — | — | — | — | 1 | 1 | — | — |
| C | — | — | — | — | 1 | — | — | — | — | — | — | — | — | — | — | — |
| HC | — | — | — | — | — | 1 | — | — | — | — | — | — | — | — | — | — |
| L | — | — | — | — | — | — | — | — | — | 2 | — | — | — | — | — | 1 |
| Re | — | — | — | — | — | — | 2 | 1 | 2 | 1 | 1 | — | — | — | — | 1 |
| Ri | — | — | — | — | — | — | — | — | 1 | — | — | — | — | — | — | — |
| T | 1 | — | 2 | — | — | — | — | — | — | — | — | 1 | — | — | — | — |
| Th | — | — | — | 1 | 1 | 2 | — | — | 2 | — | — | — | — | — | 1 | — |

TABLE 10: Edge partition for RZC_1 .

| Drugs | 0 | 1 | 2 | 3 | 4 | 5 | 6 | 7 | 8 | 9 | 10 |
|-------|---|---|----|----|----|----|----|---|---|---|----|
| A | 1 | 2 | 3 | 5 | 7 | 2 | — | 6 | 1 | 2 | 2 |
| C | — | 2 | 2 | 8 | 4 | 2 | 3 | 2 | — | — | — |
| HC | — | 1 | 3 | 7 | 5 | 2 | 3 | 2 | — | — | — |
| L | — | — | 8 | 14 | 10 | 9 | 7 | 1 | — | — | — |
| R | — | 2 | 2 | 10 | 9 | 5 | 9 | 3 | 3 | 1 | — |
| Ri | — | — | 10 | 11 | 13 | 14 | 4 | 1 | — | — | — |
| T | — | — | 2 | 5 | 4 | — | 4 | 2 | 3 | 1 | — |
| Th | — | — | 2 | 6 | 6 | 8 | 10 | 9 | 4 | 1 | — |

2.6. *Edge Partitions to Compute the Reformulated Leap Zagreb Index RZC_2 for COVID-19 Drugs.* Table 11 shows the edge partition of the considered drugs with respect to RZC_2 index.

2.7. *Edge Partitions to Compute the Reformulated Leap Zagreb Index RZC_3 for COVID-19 Drugs.* Tables 12 and 13 show the edge partition of the considered drugs with respect to RZC_3 index.

3. Curvilinear Regression and Correlation Analysis of COVID-19 Drugs

In this section, some topological indices based on Zagreb indices and some physicochemical properties which are boiling point (BP), enthalpy (E), flash point (FP), molar refraction (MR), polar surface area (PSA), polarizability (P), surface tension (T), and molar volume (MV) of antiviral drugs are analyzed.

Experimental values of physicochemical properties of the antiviral drugs presented in Table 14 were obtained from [2, 10]. We have presented the values of the proposed indices calculated using the edge partitions presented in the above section in equations (1)–(7) in Table 15.

We considered the physical properties and found the correlation between the physical properties and the four indices. In general, R^2 depicts the strength of the relationship between the dependent and independent variables. In the following, we present the linear models for only three physical properties as the correlation between the proposed indices and the rest of the properties is comparatively low. The correlation value $R^2 \geq 0.8$ and RMSE (root mean square error) metric for the predictive power of the model values are taken into consideration. The best predictive model is the minimum error, i.e., the minimum RMSE [34].

Here, we are doing a comparative analysis of the line fits. We considered the linear, quadratic, cubic, and fourth-order regression model which is also known as curvilinear regression analysis. In this paper, we examined the following equations.

The general form of the mentioned regression models is

$$P = \left[\sum_{i=1}^4 \tilde{\alpha}_i (TI)^i \right] + \bar{\gamma}, \quad (8)$$

where P is the dependent variable, $\bar{\gamma}$ is the regression model constant, and $\tilde{\alpha}_i$ are the coefficients for the topological descriptors, $i = 1, 2, \dots, 4$.

TABLE 11: Edge partition to compute RZC_2 for COVID-19 drugs.

| Edge uv with $(\tau(u), \tau(v))$ | A | C | HC | L | Re | Ri | T | Th |
|-------------------------------------|-----|-----|------|-----|------|------|-----|------|
| (1, 2) | 1 | — | — | — | — | — | — | — |
| (1, 3) | 2 | 2 | 1 | — | 2 | — | — | — |
| (2, 0) | — | — | 1 | — | — | — | — | — |
| (2, 2) | 2 | — | — | 3 | 1 | 4 | — | — |
| (2, 3) | 2 | 2 | 2 | 5 | 1 | 9 | 3 | — |
| (2, 4) | — | 2 | 3 | 2 | — | 3 | 1 | 2 |
| (2, 6) | 2 | — | — | 3 | — | — | — | — |
| (3, 3) | — | 4 | 3 | 3 | 2 | — | — | — |
| (3, 4) | 2 | 6 | 5 | 10 | 8 | 9 | 2 | — |
| (3, 5) | 2 | 1 | 2 | 2 | — | 4 | 1 | 10 |
| (3, 6) | — | 1 | — | 5 | — | 3 | 3 | 4 |
| (3, 7) | 1 | — | — | — | — | 1 | — | — |
| (4, 4) | 4 | — | 1 | 2 | — | 7 | — | 1 |
| (4, 5) | 1 | — | — | 4 | 1 | 9 | 1 | 3 |
| (4, 6) | 1 | 2 | 3 | 5 | 8 | 1 | 1 | 1 |
| (4, 7) | 3 | 1 | — | — | 2 | 1 | 2 | — |
| (4, 8) | — | — | — | — | — | — | 2 | 2 |
| (5, 5) | 1 | — | — | 6 | 2 | 6 | — | 4 |
| (5, 6) | — | 1 | 2 | 3 | 3 | 4 | 1 | 7 |
| (5, 7) | 2 | 1 | 2 | — | 2 | 2 | — | 2 |
| (5, 8) | — | — | — | — | 1 | — | — | 2 |
| (6, 6) | — | — | — | 5 | 4 | — | 1 | 5 |
| (6, 7) | 1 | 3 | 4 | — | 1 | 3 | 2 | 14 |
| (6, 8) | — | 2 | — | — | 5 | — | 2 | 2 |
| (6, 9) | 2 | — | — | 4 | 2 | — | 2 | — |
| (6, 10) | 1 | — | — | — | — | — | — | — |
| (7, 7) | — | — | 1 | — | — | 1 | — | 1 |
| (7, 8) | — | 2 | — | — | 2 | — | 3 | 3 |
| (7, 9) | 4 | — | — | — | 2 | — | — | 1 |
| (8, 8) | — | — | — | — | 1 | — | 1 | 2 |
| (8, 9) | — | — | — | — | 3 | — | 2 | 3 |
| (9, 9) | 1 | — | — | — | 1 | — | — | — |
| (9, 10) | 3 | — | — | — | — | — | — | — |

TABLE 12: Edge partition for RZC_3 .

| Drugs | (1, 1) | (2, 1) | (2, 2) | (2, 3) | (2, 4) | (2, 5) | (3, 3) | (3, 4) | (3, 5) | (3, 6) | (3, 7) |
|--------------------|--------|--------|--------|--------|--------|--------|--------|--------|--------|--------|--------|
| Arbidol | — | 2 | 3 | 4 | 3 | — | 1 | 4 | 1 | — | 2 |
| Chloroquine | 2 | — | 2 | 4 | 1 | — | 4 | 3 | 2 | 3 | — |
| Hydroxychloroquine | 1 | — | 3 | 2 | — | — | 3 | 4 | 2 | 3 | — |
| Lopinavir | — | — | 8 | 13 | 2 | — | 1 | 7 | 7 | 4 | — |
| Remdesivir | 2 | — | 2 | 8 | 2 | 2 | 2 | 6 | 2 | 5 | 1 |
| Ritonavir | — | — | 10 | 10 | 2 | — | 1 | — | 12 | 3 | 1 |
| Thalidomide | — | — | 2 | 3 | 3 | — | 2 | 1 | — | 3 | — |
| Theaflavin | — | — | 2 | 6 | 2 | — | — | 4 | 6 | 6 | 6 |

TABLE 13: Edge partition for RZC_3 (continued).

| Drugs | (4, 4) | (4, 5) | (4, 6) | (4, 7) | (4, 8) | (4, 9) | (4, 10) | (5, 8) | (5, 9) |
|--------------------|--------|--------|--------|--------|--------|--------|---------|--------|--------|
| Arbidol | — | 1 | — | 4 | 1 | 2 | 2 | — | — |
| Chloroquine | — | — | — | 2 | — | — | — | — | — |
| Hydroxychloroquine | — | — | — | 2 | — | — | — | — | — |
| Lopinavir | — | 3 | 3 | 1 | — | — | — | — | — |
| Remdesivir | 1 | 1 | 4 | 2 | 2 | — | — | 1 | 1 |
| Ritonavir | 2 | 2 | 1 | — | — | — | — | — | — |
| Thalidomide | — | — | 1 | 2 | 3 | 1 | — | — | — |
| Theaflavin | — | 2 | 4 | 3 | 4 | 1 | — | — | — |

After fitting and analyzing the regression models defined from the above equation for the physical properties based on the values of the physical properties given in Table 14 concerning each of the proposed indices whose values are provided in Table 15, we have the following observations for linear, quadratic, cubic, fourth, and fifth-order regression models.

Table 16 shows the square of correlation coefficient (R^2) obtained by cubic regression models between topological indices and physicochemical properties of various drugs used in the treatment of COVID-19 patients. Max (R^2) in Table 16 is marked in bold for each physicochemical property.

(i) In the linear regression model, the physical properties: boiling point (BP) and enthalpy (E), can be predicted using the index LM_3 . Also, the properties flash point (FP), molar refraction (MR), and polarizability (P) can be predicted using the index LEC. Furthermore, the property polar surface area (PSA) can be predicted by the index LM_1 .

$$BP = 2.6776(LM_3) + 102.11, \quad (9)$$

$$E = 0.3894(LM_3) + 21.627, \quad (10)$$

$$FP = 0.1509(LEC) + 168.39, \quad (11)$$

$$MR = 0.0583(LEC) + 57.662, \quad (12)$$

$$P = 0.02313(LEC) + 22.85, \quad (13)$$

$$PSA = 0.5107(LM_1) - 51.167. \quad (14)$$

Table 17 shows best predictive predictors, R^2 values, and RMSE values in linear regression models.

Table 18 shows the square of correlation coefficient (R^2) obtained by quadratic regression models between topological indices and physicochemical properties of various drugs used in the treatment of COVID-19 patients. Max (R^2) in Table 18 is marked in bold for each physicochemical property.

(ii) In the quadratic regression model, the physical properties: boiling point (BP), enthalpy (E), and polar surface area (PSA), can be predicted using the index LM_3 . Also, the properties flash point (FP), molar refraction (MR), and polarizability (P) can be predicted using the index LEC. Furthermore, the property surface tension (T) can be predicted by the index RZC_1 .

$$BP = 0.0039(LM_3)^2 + 0.8738(LM_3) + 284.68, \quad (15)$$

$$E = 0.0007(LM_3)^2 + 0.0668(LM_3) + 54.282, \quad (16)$$

$$FP = 4.442(10^{-5})(LEC)^2 + 0.0314(LEC) + 225.3, \quad (17)$$

$$MR = 1.463(10^{-6})(LEC)^2 + 0.0545(LEC) + 59.519, \quad (18)$$

$$P = 6.586(10^{-7})(LEC)^2 + 0.0214(LEC) + 23.681, \quad (19)$$

$$PSA = 0.002054(LM_3)^2 - 0.1345(LM_3) + 29.92, \quad (20)$$

$$T = 0.0001258(RZC_1)^2 - 0.1657(RZC_1) + 99.99. \quad (21)$$

Table 19 shows best predictive predictors, R^2 values, and RMSE values in quadratic regression models.

Table 20 shows the square of correlation coefficient (R^2) obtained by cubic regression models between topological indices and physicochemical properties of various drugs used in the treatment of COVID-19 patients. Max (R^2) in Table 20 is marked in bold for each physicochemical property.

(iii) In the cubic regression model, the physical properties boiling point (BP) and enthalpy (E) can be predicted using the index LM_3 . The properties flash point (FP) and polar surface area (PSA) can be predicted by the index LM_1 . Also, the properties molar refraction (MR), polarizability (P), and molar volume (MV) can be predicted using the index LEC. Furthermore, the property surface tension (T) can be predicted by the index RZC_2 .

$$BP = -0.0001(LM_3)^3 + 0.0928(LM_3)^2 - 19.163(LM_3) + 1692.1, \quad (22)$$

$$E = -1.711(10^{-5})(LM_3)^3 + 0.0129(LM_3)^2 - 2.684(LM_3) + 247.5, \quad (23)$$

$$FP = -5.082(10^{-5})(LM_1)^3 + 0.0515(LM_1)^2 - 15.424(LM_1) + 1656.9, \quad (24)$$

$$MR = 4.348(10^{-8})(LEC)^3 - 0.0002(LEC)^2 + 0.2912(LEC) - 20.81, \quad (25)$$

$$P = 6.586(10^{-7})(LEC)^2 + 0.0214(LEC) + 23.681, \quad (26)$$

$$PSA = -6.507(10^{-6})(LM_1)^3 + 0.0074(LM_1)^2 - 2.0905(LM_1) + 222.4, \quad (27)$$

TABLE 14: Various physicochemical properties of COVID-19 drugs.

| Drugs | BP | <i>E</i> | FP | MR | PSA | <i>P</i> | <i>T</i> | MV | IC ₅₀ |
|--------------------|--------|----------|-------|-------|-----|----------|----------|-------|------------------|
| Arbidol | 591.8 | 91.5 | 311.7 | 121.9 | 80 | 48.3 | 45.3 | 347.3 | 3.54 |
| Chloroquine | 460.6 | 72.1 | 232.3 | 97.4 | 28 | 38.6 | 44 | 287.9 | 1.38 |
| Hydroxychloroquine | 516.7 | 83 | 266.3 | 99 | 48 | 39.2 | 49.8 | 285.4 | 0.72 |
| Lopinavir | 924.2 | 140.8 | 512.7 | 179.2 | 120 | 71 | 49.5 | 540.5 | 5.25 |
| Remdesivir | — | — | — | 149.5 | 213 | 59.3 | 62.3 | 409 | 0.987 |
| Ritonavir | 947 | 144.4 | 526.6 | 198.9 | 202 | 78.9 | 53.7 | 581.7 | 8.63 |
| Thalidomide | 487.8 | 79.4 | 248.8 | 65.2 | 87 | 25.9 | 71.6 | 161 | — |
| Theaflavin | 1003.9 | 153.5 | 336.5 | 137.3 | 218 | 54.4 | 138.6 | 301 | 8.44 |

TABLE 15: Proposed topological descriptor values of COVID-19 drugs.

| Drugs | LM ₁ | LM ₂ | LM ₃ | LEC | RZC ₁ | RZC ₂ | RZC ₃ |
|--------------------|-----------------|-----------------|-----------------|------|------------------|------------------|------------------|
| Arbidol | 322 | 388 | 208 | 788 | 941 | 1496 | 494 |
| Chloroquine | 186 | 205 | 134 | 591 | 402 | 591 | 254 |
| Hydroxychloroquine | 172 | 210 | 138 | 656 | 412 | 603 | 260 |
| Lopinavir | 420 | 464 | 296 | 1934 | 844 | 1352 | 556 |
| Remdesivir | 447 | 524 | 298 | 1740 | 1113 | 1935 | 662 |
| Ritonavir | 436 | 470 | 309 | 2344 | 890 | 1254 | 584 |
| Thalidomide | 225 | 275 | 148 | 391 | 632 | 1117 | 342 |
| Theaflavin | 544 | 652 | 342 | 1622 | 1496 | 2291 | 816 |

TABLE 16: The squared of the correlation coefficient (*R*²) obtained by linear regression model between topological indices and physicochemical properties of various drugs used in treatment of COVID-19 patients.

| Index/property | BP | <i>E</i> | FP | MR | PSA | <i>P</i> | <i>T</i> | MV | IC ₅₀ |
|------------------|---------------|---------------|---------------|---------------|---------------|---------------|----------|--------|------------------|
| LM ₁ | 0.9158 | 0.912 | 0.4649 | 0.5476 | 0.8494 | 0.5477 | 0.3431 | 0.3085 | 0.5235 |
| LM ₂ | 0.8486 | 0.8484 | 0.3496 | 0.433 | 0.837 | 0.4331 | 0.4249 | 0.2089 | 0.464 |
| LM ₃ | 0.9771 | 0.9721 | 0.6071 | 0.6805 | 0.8425 | 0.6807 | 0.2479 | 0.4388 | 0.5425 |
| LEC | 0.8719 | 0.862 | 0.8856 | 0.9266 | 0.6649 | 0.9272 | 0.0332 | 0.7763 | 0.4786 |
| RZC ₁ | 0.6194 | 0.6212 | 0.1422 | 0.2241 | 0.73 | 0.2241 | 0.5445 | 0.0628 | 0.3746 |
| RZC ₂ | 0.5378 | 0.5418 | 0.1054 | 0.1603 | 0.6981 | 0.1605 | 0.4972 | 0.0345 | 0.2415 |
| RZC ₃ | 0.8211 | 0.8208 | 0.319 | 0.4084 | 0.843 | 0.4085 | 0.433 | 0.1889 | 0.4446 |

TABLE 17: Best predictive fits from linear regression model.

| Property | Curve equation | Predictor | <i>R</i> ² value | RMSE | <i>p</i> value | <i>F</i> Stat |
|----------|----------------|-----------------|-----------------------------|---------|----------------|---------------|
| BP | (9) | LM ₃ | 0.9771 | 40.0999 | 0.00291 | 29.32 |
| <i>E</i> | (10) | LM ₃ | 0.9721 | 6.4486 | 0.00004 | 174.5 |
| FP | (11) | LEC | 0.8856 | 45.4797 | 0.00157 | 38.69 |
| MR | (12) | LEC | 0.9266 | 13.017 | 0.00012 | 75.8 |
| <i>P</i> | (13) | LEC | 0.9272 | 5.1456 | 0.00012 | 76.41 |
| PSA | (14) | LM ₁ | 0.8494 | 32.1384 | 0.00113 | 33.84 |

TABLE 18: The squared of the correlation coefficient (*R*²) obtained by quadratic regression model between topological indices and physicochemical properties of various drugs used in treatment of COVID-19 patients.

| Index/property | BP | <i>E</i> | FP | MR | PSA | <i>P</i> | <i>T</i> | MV | IC ₅₀ |
|------------------|---------------|---------------|---------------|---------------|--------|---------------|---------------|--------|------------------|
| LM ₁ | 0.9158 | 0.9122 | 0.68 | 0.6475 | 0.8511 | 0.6482 | 0.7925 | 0.5197 | 0.5317 |
| LM ₂ | 0.8576 | 0.8557 | 0.6682 | 0.5944 | 0.8387 | 0.8387 | 0.8331 | 0.4976 | 0.464 |
| LM ₃ | 0.9808 | 0.9778 | 0.7248 | 0.7318 | 0.852 | 0.852 | 0.6565 | 0.5653 | 0.5809 |
| LEC | 0.9332 | 0.9196 | 0.8999 | 0.9268 | 0.6882 | 0.6882 | 0.1691 | 0.791 | 0.4854 |
| RZC ₁ | 0.6473 | 0.6468 | 0.4981 | 0.4083 | 0.752 | 0.752 | 0.8551 | 0.3563 | 0.3769 |
| RZC ₂ | 0.5474 | 0.5506 | 0.3829 | 0.2744 | 0.7019 | 0.7019 | 0.7507 | 0.237 | 0.2678 |
| RZC ₃ | 0.8331 | 0.8309 | 0.6518 | 0.581 | 0.8447 | 0.8447 | 0.8323 | 0.4919 | 0.4451 |

TABLE 19: Best predictive fits from quadratic regression model.

| Property | Curve equation | Predictor | R^2 value | RMSE | p value | F Stat |
|----------|----------------|-----------|-------------|---------|-----------|----------|
| BP | (15) | LM_3 | 0.9808 | 41.0105 | 0.000367 | 102.4 |
| E | (16) | LM_3 | 0.9778 | 6.4407 | 0.00049 | 87.97 |
| FP | (17) | LEC | 0.8999 | 47.5638 | 0.010 | 17.97 |
| MR | (18) | LEC | 0.9268 | 14.2589 | 0.00145 | 31.64 |
| P | (19) | LEC | 0.9273 | 5.6309 | 0.00142 | 31.91 |
| PSA | (20) | LM_3 | 0.8520 | 34.9049 | 0.00843 | 14.39 |
| T | (21) | RZC_1 | 0.8551 | 14.1312 | 0.00799 | 14.76 |

TABLE 20: The squared of the correlation coefficient (R^2) obtained by cubic regression model between topological indices and physicochemical properties of various drugs used in treatment of COVID-19 patients.

| Index/property | BP | E | FP | MR | PSA | P | T | MV | IC_{50} |
|----------------|---------------|---------------|---------------|---------------|---------------|---------------|---------------|---------------|---------------|
| LM_1 | 0.9923 | 0.9862 | 0.9782 | 0.8761 | 0.8636 | 0.8766 | 0.9583 | 0.8418 | 0.5515 |
| LM_2 | 0.9664 | 0.9548 | 0.9394 | 0.8025 | 0.8594 | 0.803 | 0.9653 | 0.7729 | 0.5373 |
| LM_3 | 0.9945 | 0.9899 | 0.9762 | 0.8584 | 0.8521 | 0.859 | 0.9299 | 0.8041 | 0.6358 |
| LEC | 0.9611 | 0.9537 | 0.9005 | 0.9641 | 0.7292 | 0.9644 | 0.2833 | 0.8525 | 0.5947 |
| RZC_1 | 0.6506 | 0.6477 | 0.5172 | 0.4416 | 0.7587 | 0.4424 | 0.9609 | 0.403 | 0.8215 |
| RZC_2 | 0.5544 | 0.5626 | 0.3831 | 0.2827 | 0.7055 | 0.2835 | 0.9848 | 0.2659 | 0.9534 |
| RZC_3 | 0.9395 | 0.9266 | 0.9012 | 0.7671 | 0.8713 | 0.7678 | 0.9692 | 0.7362 | 0.5494 |

$$T = 1.347(10^{-7})(RZC_2)^3 - 0.0005(RZC_2)^2 + 0.6194(RZC_2) - 165.5, \tag{28}$$

$$MV = 1.76(10^{-7})(LEC)^3 - 0.0007(LEC)^2 + 0.9903(LEC) - 107.31. \tag{29}$$

Table 21 shows best predictive predictors, R^2 values, and RMSE values in cubic regression models.

Table 22 shows the square of correlation coefficient (R^2) obtained by cubic regression models between topological indices and physicochemical properties of various drugs used in the treatment of COVID-19 patients. Max (R^2) in Table 22 is marked in bold for each physicochemical property.

(iv) In the fourth-order regression model, the physical properties: molar refraction (MR), polarizability (P), polar surface area (PSA), surface tension (T), and molar volume (MV), can be predicted using the proposed indices.

It is seen that correlations between physical properties and indices are at the best level in fourth-order regression models. It shows that we will not get a good correlation R^2 fit for all the proposed indices.

$$BP = 6.461(10^{-10})(LEC)^4 - 3.608(10^{-6})(LEC)^3 + 0.0067(LEC)^2 - 4.264(LEC) + 1336, \tag{30}$$

$$E = 1.004(10^{-10})(LEC)^4 - 5.62(10^{-7})(LEC)^3 + 0.001(LEC)^2 - 0.6791(LEC) + 216.5, \tag{31}$$

$$FP = -2.21(10^{-7})(LM_2)^4 + 0.0003(LM_2)^3 - 0.1693(LM_2)^2 + 36.76(LM_2) - 2609.6, \tag{32}$$

$$MR = -9.978(10^{-11})(LEC)^4 + 5.694(10^{-7})(LEC)^3 - 0.0011(LEC)^2 + 0.9088(LEC) - 154.5, \tag{33}$$

$$PSA = 5.706(10^{-10})(LEC)^4 - 3.086(10^{-6})(LEC)^3 + 0.0056(LEC)^2 - 3.78(LEC) + 882.3, \tag{34}$$

TABLE 21: Best predictive fits from cubic regression model.

| Property | Curve equation | Predictor | R^2 value | RMSE | p value | F Stat |
|----------|----------------|-----------|-------------|---------|-----------|----------|
| BP | (22) | LM_3 | 0.9945 | 25.2664 | 0.00068 | 182.3 |
| E | (23) | LM_3 | 0.9899 | 5.0074 | 0.00171 | 98.23 |
| FP | (24) | LM_1 | 0.9782 | 25.6428 | 0.00544 | 44.81 |
| MR | (25) | LEC | 0.9641 | 11.1621 | 0.00239 | 35.8 |
| P | (26) | LEC | 0.9644 | 4.4082 | 0.00235 | 36.09 |
| PSA | (27) | LM_1 | 0.8636 | 37.4541 | 0.03323 | 8.445 |
| T | (28) | RZC_2 | 0.9848 | 5.1180 | 0.00043 | 86.38 |
| MV | (29) | LEC | 0.8525 | 71.3318 | 0.03872 | 7.707 |

TABLE 22: The squared of the correlation coefficient (R^2) obtained by bi-quadratic regression model between topological indices and physicochemical properties of various drugs used in treatment of COVID-19 patients.

| Index/property | BP | E | FP | MR | PSA | P | T | MV | IC_{50} |
|----------------|--------------|---------------|---------------|---------------|---------------|---------------|---------------|---------------|---------------|
| LM_1 | 0.9953 | 0.9907 | 0.9937 | 0.9021 | 0.9206 | 0.902 | 0.9742 | 0.8745 | 0.5714 |
| LM_2 | 0.9964 | 0.9939 | 0.9950 | 0.9068 | 0.9211 | 0.9064 | 0.991 | 0.9042 | 0.8753 |
| LM_3 | 0.9953 | 0.9929 | 0.9921 | 0.8696 | 0.9055 | 0.8699 | 0.9452 | 0.819 | 0.6762 |
| LEC | 0.999 | 0.9967 | 0.945 | 0.9872 | 0.9835 | 0.9871 | 0.7576 | 0.9739 | 0.6315 |
| RZC_1 | 0.9378 | 0.9281 | 0.912 | 0.6986 | 0.7714 | 0.6981 | 0.9948 | 0.7044 | 0.838 |
| RZC_2 | 0.9295 | 0.9211 | 0.9002 | 0.3843 | 0.7473 | 0.384 | 0.9945 | 0.3816 | 0.9686 |
| RZC_3 | 0.9764 | 0.9728 | 0.9678 | 0.8900 | 0.9289 | 0.8896 | 0.9892 | 0.8881 | 0.8761 |

$$P = -3.93(10^{-11})(LEC)^4 + 2.243(10^{-7})(LEC)^3 - 0.0004(LEC)^2 + 0.3581(LEC) - 60.72, \tag{35}$$

$$T = -1.008(10^{-9})(RZ_1)^4 + 4.08(10^{-6})(RZ_1)^3 - 0.0057(RZ_1)^2 + 3.292(RZ_1) - 592.7, \tag{36}$$

$$MV = -7.218(10^{-10})(LEC)^4 + 3.98(10^{-6})(LEC)^3 - 0.0074(LEC)^2 + 5.458(LEC) - 1075. \tag{37}$$

From Table 23, it is clear that the proposed indices can be used to predict all the physicochemical properties of the COVID-19 drugs in the fourth-order regression models. From our analysis of the proposed indices, we observe the following:

- (i) LEC index can be used to predict the boiling point (BP), enthalpy of vaporization (E), molar refraction (MR), polar surface area (PSA), polarizability (P), and molar volume (MV) in the fourth-order regression model as the corresponding R^2 values are 0.9990, 0.9967, 0.9872, 0.9835, 0.9871, and 0.9739, respectively.
- (ii) LM_2 index can be used to predict the flash point (FP) in the fourth-order regression model as the corresponding R^2 value is 0.9950.
- (iii) RZC_1 index can be used to predict the surface tension (T) in the fourth-order regression model as the corresponding R^2 value is 0.9948.

Figures 3–5 show the plots of the fourth-order regression equations of boiling point (BP), enthalpy of vaporization (E), molar refraction (MR), polar surface area (PSA), polarizability (P), and molar volume (MV) with respect to LEC index, respectively. Figure 6 shows the plots of the fourth-order regression equations of flash point (FP) and surface tension (T) concerning LM_2 and RZC_1 indices, respectively. Figure 7 shows the plot of the fourth-order regression equation of IC_{50} with RZC_2 index.

$$IC_{50} = -2E - 11 * (RZC_2)^4 + 1E - 07 * (RZC_2)^3 - 0.0003 * (RZC_2)^2 + 0.3545 * (RZC_2) - 113.9, \tag{38}$$

with $R^2 = 0.9686$, p value = 0.06183, and F Stat = 15.42.

3.1. Multiple Linear Regression Models. In order to check the efficiency of the topological indices together, we performed the multiple linear regression models as follows:

$$\begin{aligned} \text{BP} = & -0.1064 * (\text{LEC})(\pm 0.1217) - 1.5791 * (\text{RZC}_1)(\pm 0.6084) \\ & - 0.1107 * (\text{RZC}_2)(\pm 0.1936) \\ & + 4.5195 * (\text{RZC}_3)(\pm 1.5652) + 101.3602, \end{aligned} \quad (39)$$

$$\begin{aligned} E = & -0.0173 * (\text{LEC})(\pm 0.0257) - 0.2447 * (\text{RZC}_1)(\pm 0.12841) \\ & - 0.0130 * (\text{RZC}_2)(\pm 0.0409) \\ & + 0.6812 * (\text{RZC}_3)(\pm 0.3304) + 20.5147, \end{aligned} \quad (40)$$

$$\begin{aligned} \text{FP} = & 0.3867 * (\text{LEC})(\pm 0.1029) + 0.0723 * (\text{RZC}_1)(\pm 0.5141) \\ & + 0.5741 * (\text{RZC}_2)(\pm 0.1636) \\ & - 2.4031 * (\text{RZC}_3)(\pm 1.3226) + 250.9894, \end{aligned} \quad (41)$$

$$\begin{aligned} \text{MR} = & 0.1136 * (\text{LEC})(\pm 0.0631) + 0.2799 * (\text{RZC}_1)(\pm 0.3045) \\ & + 0.0051 * (\text{RZC}_2)(\pm 0.0709) \\ & - 0.6854 * (\text{RZC}_3)(\pm 0.8186) + 85.6949, \end{aligned} \quad (42)$$

$$\begin{aligned} \text{PSA} = & 0.0985 * (\text{LEC})(\pm 0.1686) + 0.1744 * (\text{RZC}_1)(\pm 0.8143) \\ & + 0.1196 * (\text{RZC}_2)(\pm 0.1896) \\ & - 0.5668 * (\text{RZC}_3)(\pm 2.1890) - 23.9223, \end{aligned} \quad (43)$$

$$\begin{aligned} P = & 0.0453 * (\text{LEC})(\pm 0.0248) + 0.1118 * (\text{RZC}_1)(\pm 0.1198) \\ & + 0.0023 * (\text{RZC}_2)(\pm 0.0279) \\ & - 0.2746 * (\text{RZC}_3)(\pm 0.3220) + 34.0440, \end{aligned} \quad (44)$$

$$\begin{aligned} T = & -0.1592 * (\text{LEC})(\pm 0.0832) - 0.4313 * (\text{RZC}_1)(\pm 0.4019) \\ & - 0.1771 * (\text{RZC}_2)(\pm 0.0936) \\ & + 1.8107 * (\text{RZC}_3)(\pm 1.0806) - 35.1786, \end{aligned} \quad (45)$$

$$\begin{aligned} \text{MV} = & 0.4684 * (\text{LEC})(\pm 0.2798) + 1.0864 * (\text{RZC}_1)(\pm 1.3515) \\ & + 0.1532 * (\text{RZC}_2)(\pm 0.3146) \\ & - 3.3574 * (\text{RZC}_3)(\pm 3.6329) + 322.6145, \end{aligned} \quad (46)$$

$$\begin{aligned} \text{IC50} = & 0.0019 * (\text{LEC})(\pm 0.0051) + 0.0401 * (\text{RZC}_1)(\pm 0.0246) \\ & - 0.0219 * (\text{RZC}_2)(\pm 0.0062) \\ & - 0.0023 * (\text{RZC}_3)(\pm 0.0668) - 2.5597, \end{aligned} \quad (47)$$

with $R^2 = 0.9619$, p value = 0.07472, and F Stat = 12.63.

We see that the proposed indices can be used to predict all the physicochemical properties of the COVID-19 drugs through the multilinear regression models. We found that all the properties are being predicted by the mentioned

topological indices, and the corresponding R^2 and RMSE values are given in Table 24. Out of all proposed indices, we observed that these four indices, namely, LEC, RZC_1 , RZC_2 , and RZC_3 , are helpful in predicting the properties with good accuracy.

TABLE 23: Best predictive fits from bi-quadratic regression model.

| Property | Curve equation | Predictor | R^2 value | RMSE | p value | F Stat |
|----------|----------------|-----------|-------------|---------|-----------|----------|
| BP | (30) | LEC | 0.9990 | 13.5366 | 0.00938 | 105.9 |
| E | (31) | LEC | 0.9967 | 3.4841 | 0.0065 | 153.2 |
| FP | (32) | LM_2 | 0.9950 | 14.9790 | 0.00991 | 100.2 |
| MR | (33) | LEC | 0.9872 | 7.7092 | 0.00361 | 57.64 |
| PSA | (34) | LEC | 0.9835 | 15.0243 | 0.0052 | 44.83 |
| P | (35) | LEC | 0.9871 | 3.0590 | 0.00362 | 57.54 |
| T | (36) | RZC_1 | 0.9948 | 3.4504 | 0.00093 | 144 |
| MV | (37) | LEC | 0.9739 | 34.6556 | 0.01038 | 27.98 |

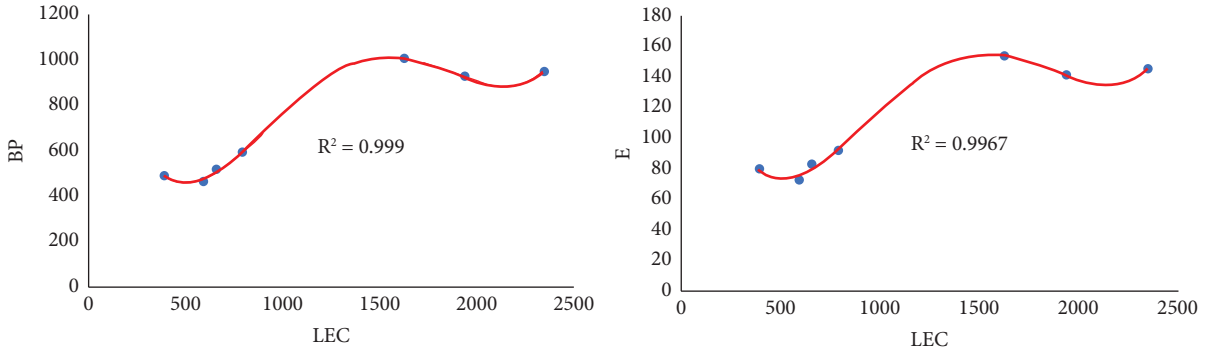


FIGURE 3: Bi-quadratic regression curves for BP and E against LEC.

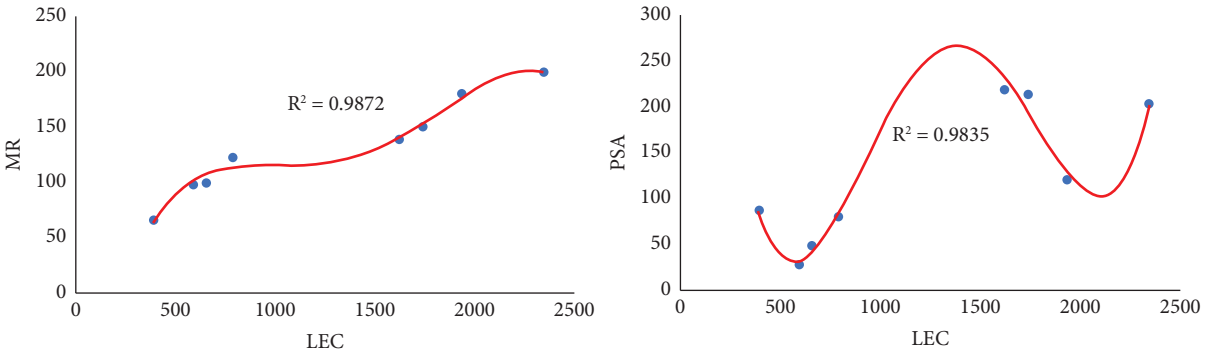


FIGURE 4: Bi-quadratic regression curves for MR and PSA against LEC.

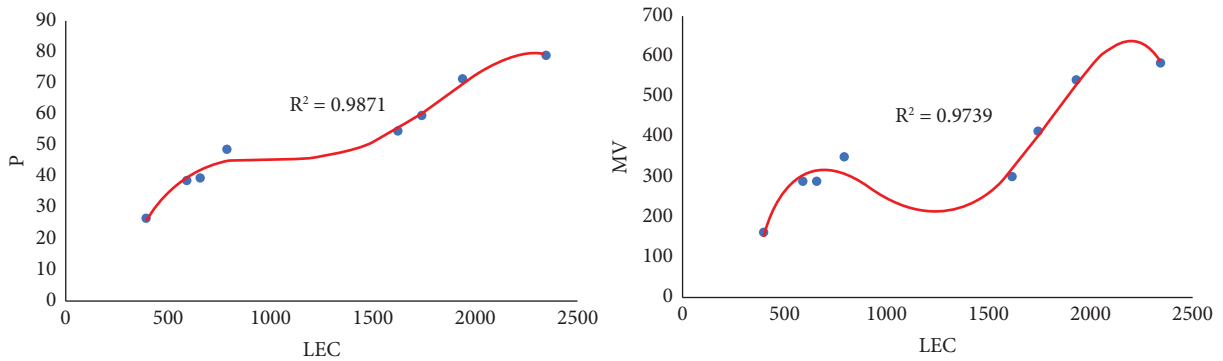


FIGURE 5: Bi-quadratic regression curves for P and MV against LEC.

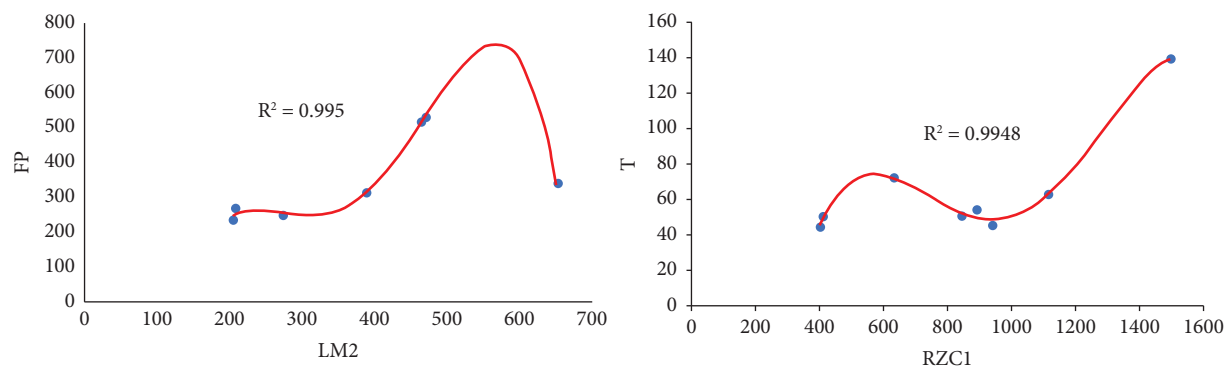
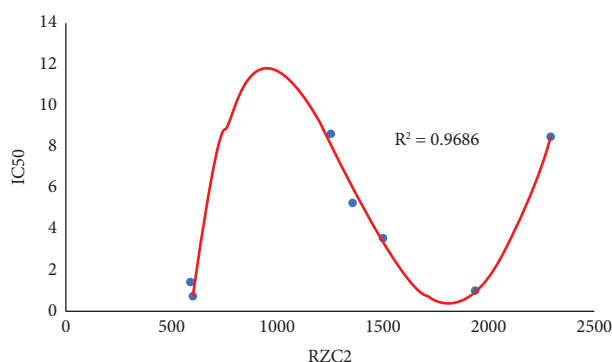
FIGURE 6: Bi-quadratic regression curves for FP and T against LM_2 and RZC_1 , respectively.FIGURE 7: Fourth-order regression curve for IC_{50} against RZC_2 .

TABLE 24: Best MLR fits.

| Property | Curve equation | R^2 value | RMSE | p value | F Stat |
|----------|----------------|-------------|---------|-----------|----------|
| BP | (39) | 0.9958 | 27.2286 | 0.0084 | 117.9 |
| E | (40) | 0.9912 | 5.7474 | 0.01762 | 55.99 |
| FP | (41) | 0.9883 | 23.0086 | 0.02329 | 42.18 |
| MR | (42) | 0.9550 | 14.2632 | 0.02244 | 16.31 |
| PSA | (42) | 0.8939 | 38.1437 | 0.08086 | 6.321 |
| P | (43) | 0.9567 | 5.6113 | 0.02193 | 16.57 |
| T | (44) | 0.8457 | 18.8286 | 0.1375 | 4.11 |
| MV | (45) | 0.9129 | 63.3038 | 0.06092 | 7.859 |

4. Conclusion

In this article, we proposed eccentricity and leap-based topological descriptors for the COVID-19 drugs, namely, Arbidol, chloroquine, hydroxychloroquine, lopinavir, remdesivir, ritonavir, thalidomide, and theaflavin.

QSPR study using curvilinear models reveals that bi-quadratic regression models provide better estimates for the physicochemical properties of the antiviral drugs utilized in the treatment of COVID-19 from Tables 17, 19, 21, and 23. Using the mentioned regression models, we see that our proposed indices are found to have a high correlation with all the physicochemical properties in the fourth order.

- (1) LEC index is best suited for predicting the boiling point (BP), enthalpy of vaporization (E), molar refraction (MR), polarizability (P), molar volume (MV), and polar surface area (PSA) in the fourth-order regression model.
- (2) LM_2 index is best suited for predicting the flash point (FP) in the fourth-order regression model.
- (3) RZC_1 index is best suited for predicting the surface tension (T) in the fourth-order regression model.

Furthermore, all features are predictable by the mentioned topological indices. On comparing with the curvilinear and multilinear models, we observed that the some of the properties are well predicted by both curvilinear and multilinear models. Overall, the bi-quadratic models are the

models with the best predictive ability when looking at the maximum R^2 and minimum RMSE. Also, bi-quadratic models have better predictive ability than multilinear models from Tables 23 and 24. With the help of the best models obtained, one can predict the physicochemical and biological activity of the drugs with similar structures.

The proposed indices can be used in designing new drugs to combat COVID-19.

Data Availability

The data used to support the findings of this study are included within the article.

Conflicts of Interest

The authors declare that they have no conflicts of interest.

Authors' Contributions

All authors contributed equally to this study.

Acknowledgments

Natarajan Chidambaram sincerely thanks Dr. Kalyani Desikan, Division of Mathematics, School of Advanced Sciences, Vellore Institute of Technology, Chennai, for allowing Vignesh Ravi to help in analyzing and improving the manuscript to its present form.

References

- [1] M. Ghorbani and M. A. Hosseinzadeh, "A new version of Zagreb indices," *Filomat*, vol. 26, no. 1, pp. 93–100, 2012.
- [2] S. A. K. Kirmani, P. Ali, and F. Azam, "Topological indices and QSPR/QSAR analysis of some antiviral drugs being investigated for the treatment of COVID-19 patients," *International Journal of Quantum Chemistry*, vol. 121, no. 9, Article ID e26594, 2021.
- [3] G. Li and E. De Clercq, "Therapeutic options for the 2019 novel coronavirus (2019-nCoV)," *Nature Reviews Drug Discovery*, vol. 19, no. 3, pp. 149–150, 2020.
- [4] M. Wang, R. Cao, L. Zhang et al., "Remdesivir and chloroquine effectively inhibit the recently emerged novel coronavirus (2019-nCoV) in vitro," *Cell Research*, vol. 30, no. 3, pp. 269–271, 2020.
- [5] D. Zhou, S. M. Dai, and Q. Tong, "COVID-19: a recommendation to examine the effect of hydroxychloroquine in preventing infection and progression," *Journal of Antimicrobial Chemotherapy*, vol. 75, no. 7, pp. 1667–1670, 2020.
- [6] J. Lung, Y. S. Lin, Y. H. Yang et al., "The potential chemical structure of anti-SARS-CoV-2 RNA-dependent RNA polymerase," *Journal of Medical Virology*, vol. 92, no. 6, pp. 693–697, 2020.
- [7] J. S. Morse, T. Lalonde, S. Xu, and W. R. Liu, "Learning from the past: possible urgent prevention and treatment options for severe acute respiratory infections caused by 2019-nCoV," *ChemBioChem*, vol. 21, no. 5, pp. 730–738, 2020.
- [8] X. Xu, P. Chen, J. Wang et al., "Evolution of the novel coronavirus from the ongoing Wuhan outbreak and modeling of its spike protein for risk of human transmission," *Science China Life Sciences*, vol. 63, no. 3, pp. 457–460, 2020.
- [9] J. Wei, M. Cancan, A. U. Rehman et al., "On topological indices of remdesivir compound used in treatment of corona virus (COVID 19)," *Polycyclic Aromatic Compounds*, vol. 42, no. 7, pp. 4300–4316, 2021.
- [10] S. Mondal, N. De, and A. Pal, "Topological indices of some chemical structures applied for the treatment of COVID-19 Patients," *Polycyclic Aromatic Compounds*, vol. 42, no. 4, pp. 1220–1234, 2020.
- [11] A. Saleh, G. S. Shalini, and B. V. Dhananjayamurthy, "The reduced neighborhood topological indices and RNM-polynomial for the treatment of COVID-19," *Biointerface Research in Applied Chemistry*, vol. 11, Article ID 11817, 2021.
- [12] V. R. Kulli, "Revan indices of chloroquine and hydroxy-chloroquine, remdesivir: research advances for the treatment of COVID-19," *International Journal of Engineering Sciences and Research Technology*, vol. 9, no. 5, pp. 73–84, 2020.
- [13] S. Nandi, B. S. Nayak, A. K. Saxena, M. K. Khede, K. K. Mayank, and K. S. Nil, "Repurposing of chemotherapeutics to combat COVID-19," *Current Topics in Medicinal Chemistry*, vol. 22, no. 32, pp. 2660–2694, 2022.
- [14] S. Nandi, M. Kumar, M. Saxena, and A. Kumar Saxena, "The antiviral and antimalarial drug repurposing in quest of chemotherapeutics to combat COVID-19 utilizing structure-based molecular docking," *Combinatorial Chemistry and High Throughput Screening*, vol. 24, no. 7, pp. 1055–1068, 2020.
- [15] S. Nandi, M. Kumar, and A. K. Saxena, "Repurposing of drugs and HTS to combat SARS-Cov-2 main protease utilizing structure-based molecular docking," *Letters in Drug Design and Discovery*, vol. 19, no. 5, pp. 413–427, 2022.
- [16] S. Nagarajan, G. Priyadharsini, and K. Pattabiraman, "QSPR modeling of status-based topological indices with COVID-19 drugs," *Polycyclic Aromatic Compounds*, pp. 1–20, 2022.
- [17] O. Colakoglu, "QSPR modeling with topological indices of some potential drug candidates against COVID-19," *Journal of Mathematics*, vol. 2022, pp. 1–9, 2022.
- [18] S. Nandi, M. Kumar, and A. K. Saxena, "QSAR of SARS-CoV-2 main protease inhibitors utilizing theoretical molecular descriptors," *Research Square*, vol. 2022, 2022.
- [19] A. M. Najji, N. D. Soner, and I. Gutman, "On leap Zagreb indices of graphs," *Communications in combinatorics and optimization*, vol. 2, no. 2, pp. 99–117, 2017.
- [20] Z. H. Shao, I. Gutman, Z. P. Li, S. H. Wang, and P. Wu, "Leap Zagreb indices of trees and unicyclic graphs," *Commun. Comb. Opt.*, vol. 3, pp. 179–184, 2018.
- [21] A. Alsinai, A. Saleh, H. Ahmed, L. N. Mishra, and N. D. Soner, "On the fourth leap Zagreb index of graphs," *Discrete Mathematics, Algorithms and Applications*, vol. 15, Article ID 2250077, 2022.
- [22] J. M. Zhu, N. Dehgard, and X. Li, "The third leap Zagreb index for trees," *Journal of Chemistry*, vol. 2019, pp. 1–6, 2019.
- [23] Z. Raza, "Leap Zagreb connection numbers for some networks models," *Indonesian Journal of Chemistry*, vol. 20, no. 6, pp. 1407–1413, 2020.
- [24] Z. Raza, "Zagreb connection indices for some benzenoid systems," *Polycyclic Aromatic Compounds*, vol. 42, no. 4, pp. 1814–1827, 2022.
- [25] V. Sharma, R. Goswami, and A. K. Madan, "Eccentric connectivity index: a novel highly discriminating topological descriptor for structure - property and structure - activity studies," *Journal of Chemical Information and Computer Sciences*, vol. 37, no. 2, pp. 273–282, 1997.
- [26] B. Goud and C. Rae, "On leap hyper-zagreb indices of some nanostructures," *International Journal of Mathematics Trends and Technology*, vol. 64, no. 1, pp. 30–36, 2018.

- [27] V. R. Kulli, "Leap indices of graphs," *Int. J. Cur. Res. Life Sci*, vol. 8, pp. 2998–3006, 2019.
- [28] V. R. Kulli, "Product connectivity leap index and ABC leap index of helm graphs," *Annals of Pure and Applied Mathematics*, vol. 18, no. 2, pp. 189–192, 2018.
- [29] V. R. Kulli, "On F-leap indices and F-leap polynomials of some graphs," *Int. J. Math. Archive*, vol. 9, pp. 41–49, 2018.
- [30] M. Ali Mohammed, R. S. H. Raad Sehen Haoer, J. Robert, N. Chidambaram, and N. Devadoss, "F-leap index of some special classes of bridge and chain graphs," *Eurasian Chem. Commun*, vol. 2, no. 7, pp. 827–833, 2020.
- [31] A. M. Naji and N. D. Soner, "The first leap Zagreb index of some graph Operations," *International Journal of Applied Graph Theory*, vol. 2, no. 1, pp. 07–18, 2018.
- [32] A. M. Naji, B. Davvaz, S. S. Mahde, and N. D. Soner, "A study on some properties of leap graphs," *Commun. Comb. Opt*, vol. 5, pp. 9–17, 2020.
- [33] P. Shiladhar, A. M. Naji, and N. D. Soner, "Computational of leap Zagreb indices of some Windmill graphs," *International Journal of Machine Intelligence and Applications*, vol. 6, no. 2, pp. 183–191, 2018.
- [34] O. C. Havare, "QSPR analysis with curvilinear regression modeling and topological indices," *Iranian Journal of Mathematical Chemistry*, vol. 10, no. 4, pp. 331–341, 2019.